RSC Advances

RSC Advances

www.rsc.org/advances

ROYAL SOCIETY OF CHEMISTRY

www.rsc.org/advances

Magnetic Nanoparticle Entrapped into the Cross-linked Poly(imidazole/imidazolium) Immobilized Cu(II): An Effective Heterogeneous Copper Catalyst

Ali Pourjavadi,*[a] Seyed Hassan Hosseini,[a] and Nasrin Zohreh[b], Craig Bennett[c]

[a] *Polymer Research Laboratory, Department of Chemistry, Sharif University of Technology, Tehran, Iran*
[b] *Department of chemistry, Faculty of Science, University of Qom, P. O. Box: 37185-359, Qom, Iran*
[c] *Department of Physics, Acadia University, Wolfville, Nova Scotia, Canada*

(E-mail address: purjavad@sharif.edu; Phone/fax: (982)166165311)

Abstract: Anchoring of copper sulfate in layered poly(imidazole-imidazolium) coated magnetic nanoparticles provided a highly stable, active, reusable, high loading, and green catalyst for click synthesis of 1,2,3-triazoles via one-pot cycloaddtion of alkyl halide, azide, and alkyne (Cu-A^{3}C). The catalyst was characterized by FTIR, TGA, TEM, SEM, XRD, EDAX, VSM and AAS. High selectivity, broad diversity of alkyl/benzyl bromide/chloride and alkyl/aryl terminal alkynes, and good to excellent yields of products were obtained using 0.7mol% catalyst. The catalyst was readily recovered and reused up to 6 times without significant loss of activity.

Keywords: Poly imidazolium, Magnetic nanoparticles, Click chemistry

1

INTRODUCTION

Several features of copper confer a remarkably broad range of activities allowing it to catalyze the oxidation and oxidative union of many substrates. [1]

To date, numerous copper-based catalytic systems have been reported for various organic transformations.[1-4] However, in recent years, heterogenization of copper has received considerable attention through supporting or immobilizing the catalyst into or onto the insoluble solid support. Some of the most important heterogeneous Cu-catalyzed processes reported in recent years, include self-condensation of amines,[5] C-H arylation,[6,7] asymmetric Henry reaction,[8,9] terminal alkyne homocoupling,[10,11] kinetic resolution of 1,2-diols,[12,13] Ulmann type C-X cross-coupling,[14-16] chemoselective hydrogenation of cinnamaldehyde,[17] Sonogashira reaction,[18,19] alcohol oxidation,[20] epoxidation of alkenes,[21,22] addition of terminal alkynes to imines,[23-26] and, perhaps the most important, Cu-azide-alkyne cycloaddition (CuAAC) reaction resulting in 1,2,3-triazoles known as a click reaction.

The primary advantages of these heterogeneous copper-based catalysts, as opposed to homogeneous ones, are easy catalyst recyclability and product separation, minimizing waste of the products during the catalyst separation and its disposal.[24,16] In addition, the recycled catalyst can be reused for several runs[10] reducing the cost of production[12]. Robustness, increased air, moisture and thermal stability[14], minimization of metal leaching[21,25] , improved handling of the catalyst[8] and minimization of product contamination with copper[27] are other advantages of heterogeneous copper-based catalysts.

Following the Sharpless's report [28] on Cu catalyzed azide-alkyne cycloadditon (CuAAC) and considering the advantages of heterogeneous catalysts, various heterogeneous systems have been attained by the covalent and non-covalent immobilization of copper onto the variety of supports

for CuAAC. Most include supported Cu^0 nanoparticles on solid supports[29] such as Al_2O_3/ball-milling,[30] chelate resins,[31] silica coated maghemite,[32] and nano Fe_3O_4/glutathione.[33] Moreover, various N- or C-ligand/Cu^I complexes have been covalently immobilized on solid supports for CuAAC.[34] Magnetic or silica supported ionic liquid/NHCs,[35,36] dendrimers,[37] polymer-supported azide or 2,2'-biarylpyridine,[38,39] magnetic chelating adsorbents,[40] merrifield resin supported tris(triazolyl)methanol,[41] SiO_2 supported immino pyridine,[42] and supported copper(I)–NHC[43] are some examples. Although, these catalysts are efficient, each of them suffers from some drawbacks such as multi-step catalyst preparation, low loading, long reaction time, tedious work up of catalyst and product, and harsh reaction condition. In most cases, the low loading problem of heterogeneous Cu-catalysts leads to the application of a larger amount of catalyst or higher temperature and longer reaction time. Immobilization of Cu onto the surface of polymers is a good way to overcome this limit since a large number of functionalities can be linked to Cu.

Accordingly, with the aim of increased ease of recovery, increased loading and stability of catalyst, and effective anchoring, we have investigated the development of novel cross-linked poly(imidazole/imidazolium)-Cu^{II} coated magnetic nanoparticles and its efficiency in copper-catalyzed alkyl halide-azide-alkyne cycloaddition (Cu-A^3C) as a one-pot three-component "click reaction" for synthesis of 1,2,3-triazoles.

EXPERIMENTAL

Reagents and analysis

Ferric chloride hexahydrate ($FeCl_3.6H_2O$), ferrous chloride tetrahydrate ($FeCl_2.4H_2O$), copper sulfate ($CuSO_4$), ammonia (30%), and 3-methacryloxypropyltrimethoxy silane (MPS, 98%) were purchased from Merck. 1-Vinylimidazole was obtained from Aldrich and was distilled before

use. 1,4-Dibromobutane was obtained from Aldrich, while 2,2′-azobisisobutyronitrile (AIBN, Kanto, 97%) was recrystallized from ethanol.

FTIR spectra of samples were taken using an ABB Bomem MB-100 FTIR spectrophotometer. Thermogravimetric analysis (TGA) was performed under a nitrogen atmosphere using a TGA Q 50 thermogravimetric analyzer. The morphology of the catalyst was observed using a Philips XL30 scanning electron microscope (SEM) and transmission electron microscopy (TEM) images were taken using a Philips CM30 electron microscope.

Synthesis of vinyl functionalized magnetic nanoparticles

The magnetic Fe_3O_4 nanoparticle coated silica (denoted as MNP) was synthesized as previously reported method.[44]

1 g MNP was added to dry ethanol and then 2 mL of ammonia solution was added to the flask. An excess amount (10 mmol) of the 3-(trimethoxysilyl)propylmethacrylate (MPS) solution was then dropwise added and the mixture was stirred at 60 °C for 48 h. The MPS coated magnetic nanoparticles (denoted as MNP@MPS) were magnetically separated and washed several times with methanol and dried under vacuum at 50 °C.

Synthesis of IL monomer and cross-linker

Typically, 1-vinylimidazole (2.82 g, 30 mmol) and ethyl bromide (3.27 g, 30 mmol) were stirred in 10 mL methanol at 60 °C for 20 h. The reaction mixture was then cooled to room temperature and added to 250 mL of diethyl ether. The resulting translucent solution was placed in a refrigerator for 5 h. Solid products were separated by decantation of supernatant and washed three times with diethyl ether and dried under vacuum at 50 °C. For exchange of bromide anion to tetrafluoroborate, 3-ethyl-1-vinylimidazolium bromide was stirred in an equimolar amount of aqueous HBF_4 (50%) at room temperature. The pure product was obtained after evaporation of

water at 70 °C under reduced pressure. The same procedure was used for the synthesis of 1,4-butanediyl-3,3′-bis-1-vinylimidazolium bistetrafluoroborate ([BBVim][BF$_4$]$_2$) except that the molar ratio of 1-vinylimidazole to 1,4-dibromobutane and HBF$_4$ to 1,4-butanediyl-3,3′-bis-1-vinylimidazolium dibromide were 2:1. ^{1}H and ^{19}F NMR of the monomer and cross-linker are cited in the supporting information.

Synthesis of the catalyst

MNP@MPS (0.4 g), 1-vinylimidazole (Vim, 1g), IL monomer ([EVim][BF$_4$], 0.4 g) and cross-linker ([BBVim][BF$_4$]$_2$, 0.2 g) were loaded into a 50 mL round bottom flask and 30 mL of methanol was added. The mixture was sonicated for 20 min and then deoxygenated by argon for another 20 min. Afterwards, AIBN (0.1 g) was added to the mixture and the flask was equipped with a condenser and placed in an oil bath at 70 °C. After 18 h, the solid products were magnetically separated and washed three times with methanol and dried under vacuum at 50 °C (MNP@PIL, 1.37g).

The resulting powdered materials were subjected to an anchoring (complexation) reaction. The powdered magnetic PIL (0.5 g) was added to 30 mL water and an excess amount of CuSO$_4$ (1.5 g) was added to the solution. The mixture was vigorously stirred for 3 days at 70 °C. The solid products (MNP@PILCu) were then magnetically separated, washed five times with water (5 × 100 mL) and twice with methanol (2 × 20 mL) and dried under vacuum at 50 °C.

General procedure for CuAAC reaction catalyzed by MNP@PILCu

Deionized water (2 mL) and Na-ascorbate solution (1 mL, 20 mol%) was added to a mixture of alkyne **1** (1 mmol), halide **2** (1 mmol), NaN$_3$ (1.3 mmol) and MNP@PILCu (4 mg, 0.7 mol% Cu) in a round-bottom flask (10 mL). The reaction mixture was then stirred at 50 °C for an appropriate time indicated in Table 3. After reaction completion, methanol was added and the

catalyst was magnetically separated, washed with methanol and dried for another run. The product mixtures were extracted by hot ethyl acetate and obtained as almost pure crystals after removal of the solvent under reduced pressure. The structures of the products were confirmed by physical property measurements and spectral data (see supporting information).

RESULTS and DISCUSSION

The desired catalyst was prepared via a few steps. Magnetic nanoparticles were prepared based on co-precipitation of a mixture solution of Fe(II) and Fe(III) in alkaline pH. This method produces Fe_3O_4 nanoparticles with sufficient magnetism to allow easy catalyst recovery. Coating of the Fe_3O_4 surface with a SiO_2 shell was carried out by TEOS to increase stability against acidic medium and to provide easier functionalization in the next synthesis steps. In order for effective polymerization and covalent grafting of copolymers onto the surface, MNPs were subjected to functionalization with MPS before polymerization. The presence of functional group C=C in MPS facilitated this approach.

Ionic liquid monomer 3-ethyl-1-vinylimidazolium tetrafluoroborate ([EVim][BF_4]) and cross-linker 1,4-butanediyl-3,3′ -bis-1-vinylimidazolium bistetrafluoroborate ([BBVim][BF_4]$_2$) were prepared by quaternization of 1-vinylimidazole with ethyl bromide followed by exchange of the bromide with BF_4 anion. The copolymerization and grafting was carried out by free radical initiation polymerization of monomers in the presence of MNP@MPS and cross-linker (Scheme 1). Copolymerization was initiated by AIBN and magnetic nanoparticles were entrapped into the cross-linked insoluble copolymers. This approach efficiently endows the resulting MNP@PIL particles with a series of active catalyst sites, providing higher catalyst loading. Finally, copper was loaded via complexation of copper sulfate and copolymer chains on the surface of

MNP@PIL. This resulted in the desired magnetic poly(imidazole/imidazolium)-immobilized Cu^{II} (MNP@PILCu).
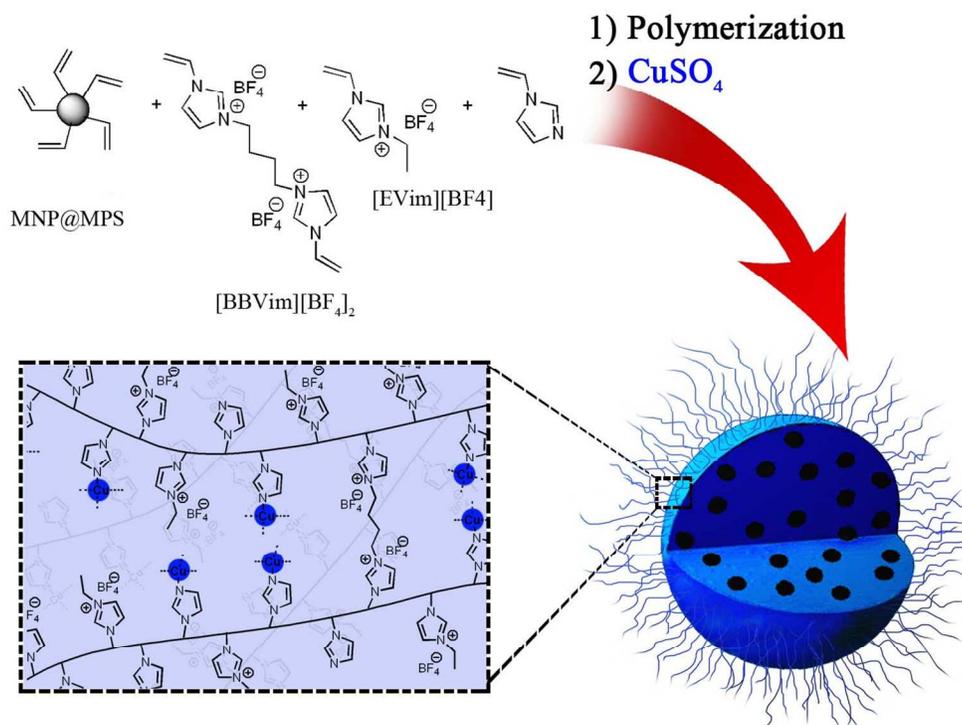
Scheme 1. Preparation of MNP@PILCu catalyst

Due to the polymer coating, the catalyst adsorbs more copper ions than traditional heterogeneous catalysts. Also, the polymer chains on the surface of the catalyst increase the spacer length and the substrates can easily adsorb onto the catalyst surface. Moreover, the ionic part of the copolymer in the MNP@PIL structure accelerates the substrate adsorption onto the catalyst surface and the reaction proceeds faster. The hydrophobic BF_4^- anions in copolymer matrix prevent the swelling of the catalyst in water medium and reduce the copper ion leaching.

FTIR was employed to characterize the catalyst at this step. As shown in Fig. 1, FTIR spectrum of MNP (Fig. 1a), MNP@MPS (Fig. 1b), MNP@PIL (Fig. 1c), and MNP@PILCu catalyst (Fig. 1d) shows stretching mode vibrations of Fe-O and Si-O in the same region around 640 and 1100

cm^{-1}, respectively. Coating of MPS onto the MNP surface was confirmed by stretching mode

vibrations of C=C and steric C=O at 1420 and 1720 cm^{-1} in the FTIR spectrum of MNP@MPS

(Fig. 1b). After copolymerization, MNP@PIL showed a strong band at 3100 cm^{-1} as well as

bands at 1610 and 1530 cm^{-1}, clearly indicating the presence of aliphatic C-H and imidazole ring.

On complexation with copper, the FTIR spectrum of MNP@PILCu (Fig. 1d) showed a new band

at 1120 cm^{-1} attributed to the S=O bond of CuSO$_4$. These results confirm that catalyst was
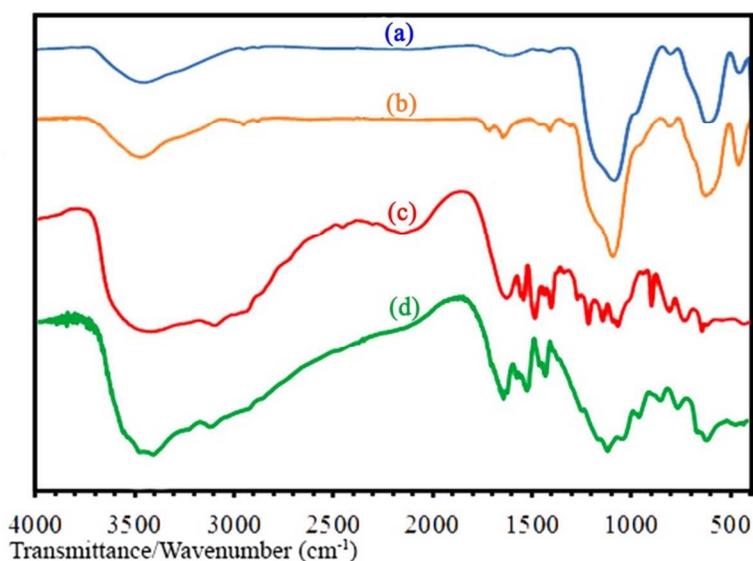
successfully prepared.

Fig. 1. FTIR spectra of MNP (a), MNP@MPS (b), MNP@PIL (c) and MNP@PILCu (d).

The thermal stability and organic content of MNP@PIL was measured by thermal gravimetric

analysis (Fig. 2). The weight loss for all samples occurring around 150 °C was completely

attributed to the loss of adsorbed water molecules. Comparison of the weight losses in the TGA

curves of MNP (Fig. 2a) and MNP@MPS (Fig. 2b) showed that loading of MPS on the surface

of MNP is 0.78 mmolg^{-1}. From the TGA curve of MNP@PIL, it was calculated that the

copolymer content in the catalyst is about 55 wt%. It is notable that the loading amount of the

monomer and the cross-linker cannot be calculated individually by TGA due to the identical nature of monomer and cross-linker. DTG analysis shows three peaks at 100, 320 and 380 °C which are attributed to weight losses for losing adsorbed water molecules, imidazolium and imidazole parts of the catalyst structure, respectively. These results showed that catalyst is thermally stable and can be used under harsh reaction condition at high temperature.
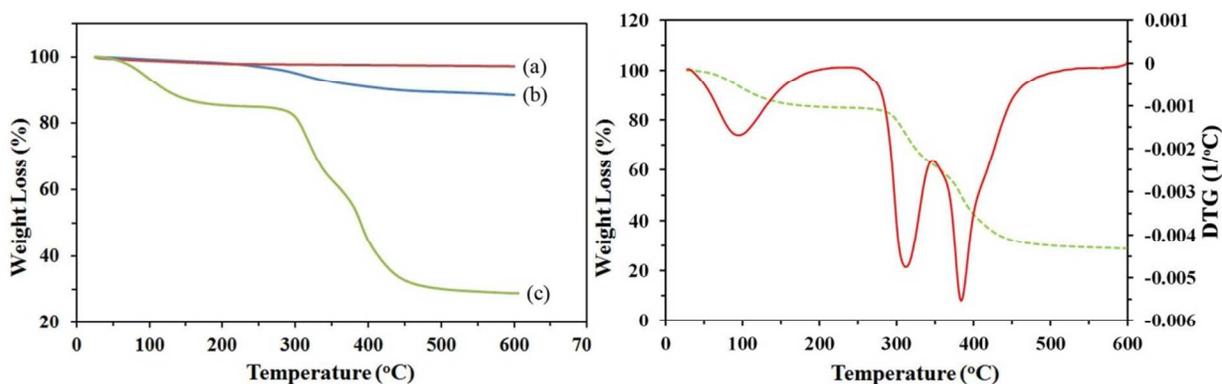
Fig, 2. TGA and DTG curves of MNP (a), MNP@MPS (b) and MNP@PIL (c).

Fig. 3 displays the powder x-ray diffraction patterns collected over the two-theta range 5 to 100 degrees for MNP@PILCu. The diffraction peaks have similar positions and relative intensities as the standard Fe_3O_4 sample (blue lines) showing that the modifications have not caused a phase change in the Fe_3O_4 particles. A broad peak around 20° is attributed to the amorphous silica shell around the magnetic nanoparticles.
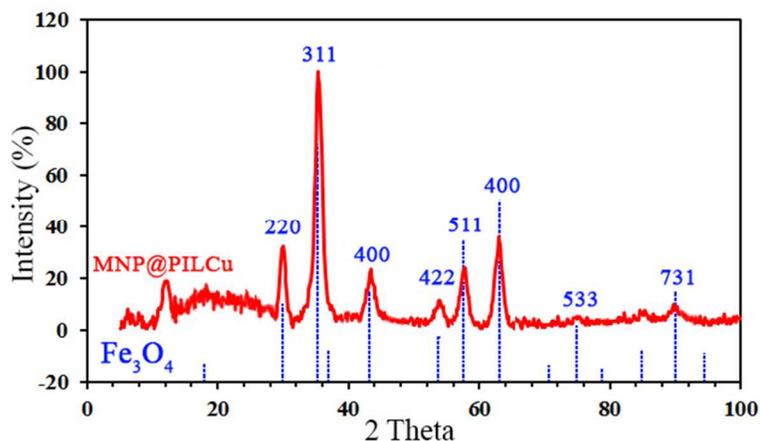
Fig. 3. The XRD pattern of MNP@PILCu.

The magnetization curves of MNP and MNP@PILCu showed small coercivities, which indicated the superparamagnetic nature of both materials (Fig. 4). The saturation magnetization of MNP@PILCu is smaller than bare MNP due to entrapment of MNPs into the nonmagnetic materials. However, the magnetization is still large enough for separation of the catalyst.
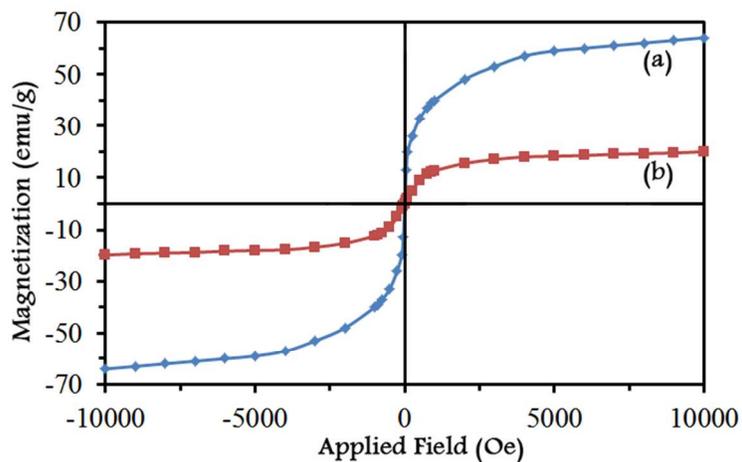

Fig. 4. Magnetization curves of MNP (a) and MNP@PILCu (b).

The TEM image of magnetic nanoparticles and MNP@PILCu are shown in Fig. 5a and b, respectively. TEM image of the catalyst showed the presence of well dispersed spherical nanoparticles into the copolymer matrix. The average size of the magnetic nanoparticles was observed to be 3.0 ± 0.8 nm, reflecting a narrow size distribution in the catalyst.

Fig. 5. TEM images of MNP@PILCu
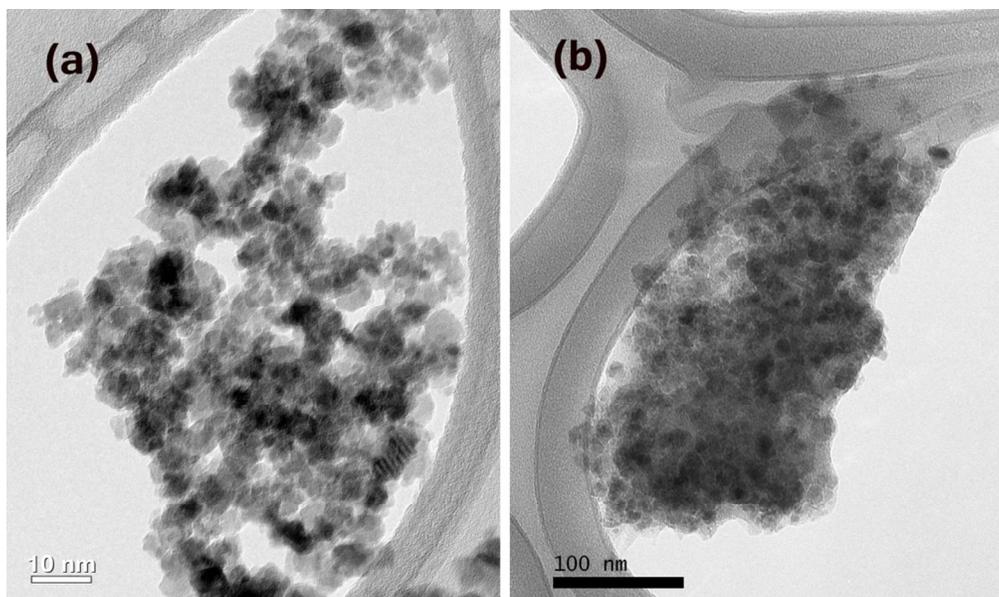
A typical SEM image and EDX analysis of MNP@PILCu is shown in Fig. 6. A bulk polymeric structure with a rough surface is seen in SEM image. The rough surface of the catalyst is due to the presence of the magnetic nanoparticles. Such a structure increases the catalytic surface area and improves the catalytic activity. EDX analysis confirms the presence of copper and iron in the catalyst.
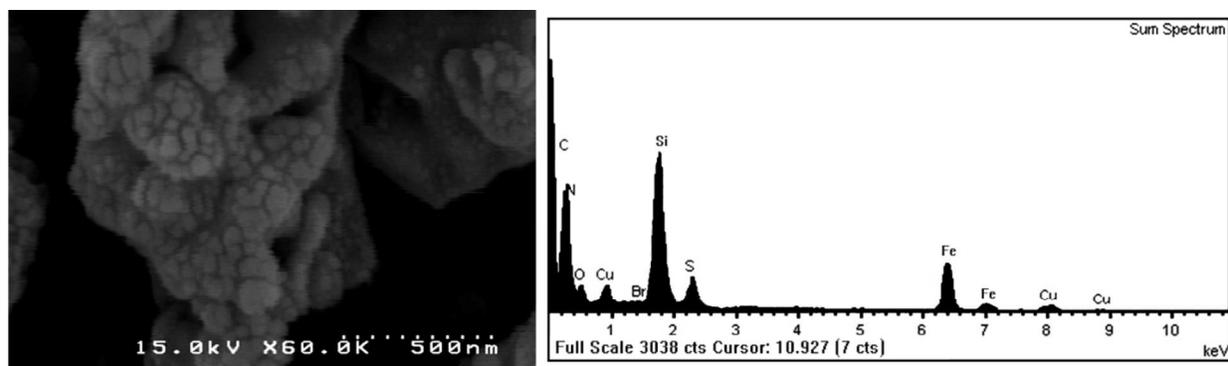
Fig. 6. SEM image and EDAX analysis of MNP@PILCu.

The loading of Cu(II) ions in MNP@PILCu was calculated by atomic absorption spectroscopy (AAS) using standard samples. It was found that the loading amount of Cu(II) ions in MNP@PILCu is 1.87 mmol g^{-1}. This result shows that catalyst has high loading level of copper ions.

One-pot cycloaddition reaction of benzyl bromide, sodium azide and phenyl acetylene in the presence of Na-ascorbate, was selected as a click model reaction to investigate the efficiency of the MNP@PILCu catalyst. Several optimizations, such as catalyst loading , NaN_3 and Na-ascorbate amount, solvent, temperature, and time were examined to obtain the best catalytic condition for click synthesis of *N*-benzyl-4-phenyl-1,2,3-triazole. Water clearly stands out as the solvent of choice because of its low cost, green nature and environmental acceptability. Thus, optimization of catalyst amount, temperature, and time were carried out in H_2O as solvent using equimolar ratio of reactant and 10 mol% Na-ascorbate (Table 1). It was found that the amount of catalyst, except when present in very low quantity (entries 12,13), is inversely related to the reaction temperature and time. Thus, in order to avoid long reaction time and high temperature, the use of 4 mg MNP@PILCu at 50 °C was selected for further optimization of the model

12

reaction. Under this condition, increasing the amount of NaN_3 and Na-ascorbate from 1 to 1.3 eq

and 10 to 20 mol%, enhanced the yield of product **3a** up to 95% (entry 8). Other solvents were

also tested (entries 14-20). In aprotic polar and nonpolar solvent, the reaction gives very low

yield probably because of poor solubility of NaN_3. In polar protic solvents, reactions take place

at higher rate with more than 70% yield of product. However it was found that H_2O functioned

better than other protic solvents, probably because of its high ability to dissolves NaN_3.

Table 1. Optimization of reaction conditions for the click Cu-A^{3}C reaction[a]
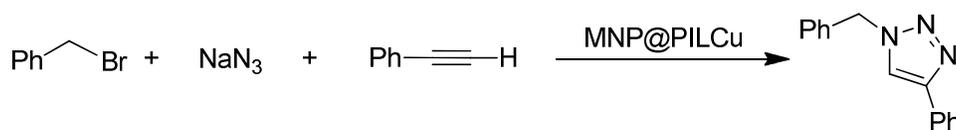
Entry	Solvent	Catalyst (mg)	T (°C)	Time (h)	NaN_3 (eq)	Na ascorbate (mol%)	Yield (%)[b]
1	H_2O	10	r.t	3	1	10	81
2	H_2O	6	r.t	4	1	10	88
3	H_2O	4	r.t	4	1	10	70
4	H_2O	4	r.t	7	1	10	91
5	H_2O	4	50	2	1	10	89
6	H_2O	4	80	2	1	10	91
7	H_2O	4	50	2	1.3	10	92
8	**H_2O**	**4**	**50**	**2.5**	**1.3**	**20**	**95**
9	H_2O	4	50	3	1.3	20	95
10	H_2O	5	50	3	1.3	20	95
11	H_2O	5	50	4	1.3	20	96
12	H_2O	3	50	4.5	1.3	20	83
13	H_2O	2	50	5	1.3	20	63
14	neat	4	50	5	1.3	20	40
15	^{t}BuOH	4	50	3	1.3	20	70
16	^{t}BuOH:H_2O (1:4)	4	50	3	1.3	20	75
17	DMF	4	50	2.5	1.3	20	64
18	CH_3CN	4	50	2.5	1.3	20	21
19	CH_2Cl_2	4	50	2.5	1.3	20	trace
20	THF	4	50	2.5	1.3	20	10

[a] Benzyl bromide: 1 mmol, phenyl acetylene: 1 mmol, solvent: 2 mL.
[b] Isolated yield.

For further investigation in catalyst activity same reaction under optimized condition was performed in the presence of 1mol% copper sulfate as a catalyst. The result showed that the yield of triazole product was 12% (1:1 mixture of regioisomers). A second reaction was also performed by copper sulfate in the presence of 10 mol% 1-methylimidazol as a ligand. The result showed that the yield of triazole product increased to 98% (pure regioisomer). These results show that imidazole groups improve the activity and selectivity of copper catalyst by complexation.

Under the optimized reaction condition, the scope of the copper catalyzed synthesis of 1,2,3-triazole with respect to the various acetylenes and halides was explored. As indicated in Table 3, both aromatic and aliphatic terminal acetylenes gave the corresponding triazoles in good yields. However aliphatic alkynes required longer reaction times compared to their aryl counterparts (compare 16/1, 17/2, 20/1, 18/8). More importantly, electron-deficient acetylenes (entries 13-15) which are normally difficult substrates for Cu-A^{3}C, exhibited similar behavior and led to triazole formation in high yield with acceptable reaction times. A variety of halide substrates were also subjected to the Cu-A^{3}C click reaction. It was found that all reactions produced corresponding triazoles, however, the reaction rates of chlorides (entries 1,3,7,10) were slower than bromides, so that the reaction time must be enhanced for an equivalent transformation. It was also found that the benzyl halides containing electron-donating groups (compare entries 1,3,4) gave the products in lower yields or longer reaction times. These results indicate that the catalytic systems can be readily applied to the combinatorial click synthesis of 1,4-disubstitiuted-1,2,3-triazoles.

14

Table 3
Three-component click synthesis of 1,2,3-triazoles using MNP@PILCu catalyst[a]

$$R-X \ + \ NaN_3 \ + \ R'{\equiv}H \ \xrightarrow[\substack{Na\ ascorbate\ (20\ \%mol)\\H_2O,\ 50\ ^oC}]{MNP@PILCu\ (4\ mg)} \ \underset{3}{R-N\overset{N=N}{\diagdown}R'}$$
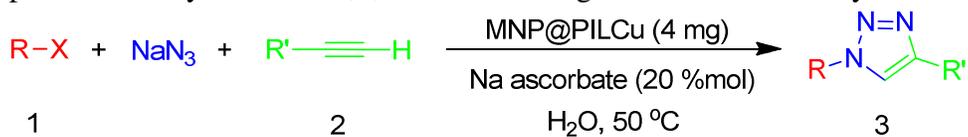
Entry	1	2	Time (h)	yield of 3 (%)[b]
1	Ph–X	Ph≡H	2.5 (X =Br) 3 (X = Cl)	3a: 95 3a: 94
2	Cl–C₆H₄–CH₂Br	Ph≡H	3	3b: 91
3	Me–C₆H₄–CH₂X	Ph≡H	2.5 (X = Br) 3.5 (X = Cl)	3c: 92 3d: 89
4	O₂N–C₆H₄–CH₂Br	Ph≡H	2	3e: 97
5	~~Br	Ph≡H	4	3f: 88
6	Br~~Br	Ph≡H	4	3g: 87
7	~~~X	Ph≡H	4 (X = Br) 4 (X = Cl)	3h: 84 3h: 80
8	PhC(O)CH₂Br	Ph≡H	3	3i: 90
9	EtO₂C-CH₂CH₂-Br	Ph≡H	3.5	3j: 91
10	allyl–X	Ph≡H	2.5 (X = Br) 3 (X = Cl)	3k: 93 3K: 90
11	naphthyl-CH₂Cl	Ph≡H	4	3l: 90
12	CH(Ph)OTs	Ph≡H	4	3a: 96
13	Ph–Br	MeO₂C≡H	4	3m: 90[c]
14	Me–C₆H₄–CH₂Cl	MeO₂C≡H	4	3n: 91[c]
15	Ph–Br	EtO₂C≡H	4	3o: 94[c]
16	Ph–Br	~~~≡H	3	3p: 87

15

17	Cl—C6H4—CH2Br	(alkyne 1) H	2.5	**3q**: 90
18	Ph—C(=O)—CH2Br	(alkyne 2) H	3.5	**3r**: 88
19	Ph—C(=O)—CH2Br	HO—CH2—C≡C—H	3	**3s**: 90
20	Ph—CH2Br	HO—CH2—C≡C—H	3	**3t**: 92

[a] Reaction condition: alkyl halide (1 mmol), NaN$_3$ (1.3 mmol), acetylene (1 mmol), H$_2$O (2 mL).
[b] Isolated yield.
[c] MeOH as solvent.

Metal leaching is an important issue to consider when working with metal-supported heterogeneous catalysts, it being necessary to verify whether the observed catalyst activity is derived from solid or leached metal species to the solution. To determine whether our click reaction using MNP@PILCu actually occurs through a heterogeneous catalytic process, the following experiments were carried out. The model reaction was performed under optimized condition (Table 1, entry 8), and the MNP@PILCu catalyst was completely removed from the reaction mixture by an external magnet after 60 min. Then, the reaction was allowed to stir for 4 hours (Figure 7) and it was found that no further production of **3a** was observed. After catalyst removal, the reaction mixture was also analyzed using induction coupled plasma (ICP-AES) and no copper species were detected. These results can rule out any contribution of leached copper into the reaction medium, and confirms that the observed catalyst is completely heterogeneous.
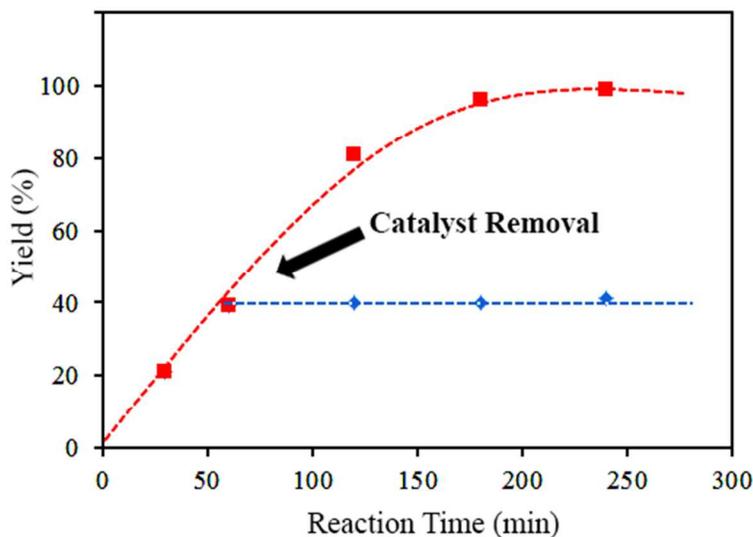
16

Fig. 7. Leaching experiment. Red line: reaction in the presence of catalyst and Blue line: reaction after removal of catalyst

The most important factors concerning a heterogeneous catalyst are its stability and reusability under the reaction conditions along with the ease of separation. To investigate these factors for MNP@PILCu, benzyl bromide, phenyl acetylene and sodium azide were subjected to the click reaction in the presence of catalyst MNP@PILCu under optimized condition. The catalyst was easily recovered and reused up to 6 times. As depicted in Fig. 8, the catalytic system worked extremely well even up to six subsequent runs with almost 92% yield and without significant loss of activity. According to the leaching experiments, a slight decrease in the yield was attributed to the loss of catalyst mass within the recovery and washing process. The TEM images of the catalyst after recovery (Fig. S1) showed that the structure of the catalyst was stable under the reaction conditions with no change being observed. The FTIR spectrum of the catalyst after recycling showed all the characteristic peaks of fresh catalyst, except the stretching vibration peak of the sulfate anions of copper sulfate which are exchanged by ascorbate.
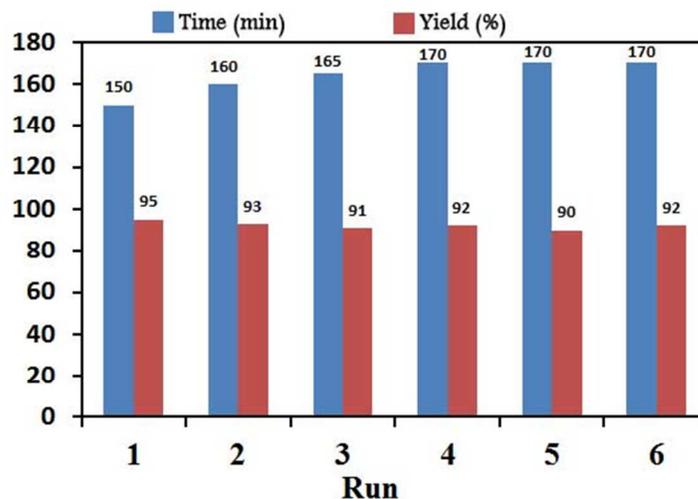
17

Fig. 8. Recycling experiment

A comparison between MNP@PILCu and other reported supported copper catalysts is presented at Table 3. As shown in table 3, copper loading in MNP@PILCu is higher than other catalysts due to imidazole groups strongly adsorb copper ions from the solution. Also, the amount of applied catalyst in the reaction was mostly lower than other catalysts. These results show that the presence catalyst has some advantage than other reported copper catalysts.

Table 3. The comparison of MNP@PILCu with reported catalysts in the synthesis of triazoles

Catalyst	Copper Loading on Catalyst (mmol/g)	Catalyst Loading (mol%)	Time (h)	T (^{o}C)	Yield (%)	Ref
Functionalized Chitosan/Cu	0.6	0.1	12h	70	99	[45]
Cross-linked poly(IL)/Cu	1.0	1.0	48h	r.t	98	[46]
Ionic Polymer /Cu	0.25	5	2.5h	r.t	99	[47]
Poly(4-vinyl pyridine)/Cu	1.32	13	25 min	100	89	[48]
Nano ferrite-glutathione-copper	0.25	2.5	10min	120 mw	99	[49]
Poly(NIPAM/Im)/Cu	0.46	0.25	1.5	50	99	[50]
MNP@PILCu	1.87	0.7	25 min	50	95	Present work

CONCLUSION

In conclusion, we have successfully developed a novel environmentally friendly magnetic poly(imidazole/imidazolium)-supported Cu(II) for the synthesis of 1,4-disubstituted-1,2,3-triazoles via one pot three-component reaction of alkyl/benyl halide, sodium azide and terminal alkyne known as click reaction. The reaction is simple to perform and is not sensitive to moisture and oxygen. This procedure is applicable to both aromatic/aliphatic acetylenes and alkyl/benzyl halides, and generates a diverse range of triazoles in excellent yields. High loading level of Cu(II) on the surface of polymer-supported MNP leads to the use of a small quantity (4 mg) of catalyst in each reaction. The relatively simple preparation procedure, easy magnetic recovery and excellent reusability (up to 6 runs) is expected to contribute to the utilization of this catalyst for the development of benign chemical processes and products.

REFERENCES

1- S. E. Allen, R. R. Walvoord, R. Padilla-Salinas, M. C. Kozlowski. *Chem. Rev*., 2013, **113** (8), 6234-6458.

2- A. Alexakis, J. E. Bäckvall, N. Krause, O. Pamies, M. Dieguez, *Chem. Rev*., 2008, **108**, 2796-2823.

3- S. Reymond, J. Cossy, *Chem. Rev*., 2008, **108**, 5359-5406.

4- G. Evano, N. Blanchard, M. Toumi, *Chem. Rev*., 2008, **108**, 3054-3131.

5- I. Kim, S. Itagaki, X. Jin, K. Yamaguchi, N. Mizuno, *Catal. Sci. Technol*., 2013, **3**, 2397-2403.

6- A. Honraedt, F. Le Callonnec, E. Le Grognec, V. Fernandez, F. Felpin, *J. Org. Chem*., 2013, **78** (9), 4604-4609.

7-   J. Albadi, F. Shirini, J. Abasi, N. Armand, T. Motaharizadeh, *Comptes Rendus Chimie* 2013, **16**, 407-411.

8-   J. M. Lee, J. Kim, Y. Shin, C. E. Yeom, J. E. Lee, T. Hyeon, B. M. Kim, *Tetrahedron: Asymmetry* 2010, **21**, 285-291.

9-   K. Dhahagani, J. Rajesh, R. Kannan, G. Rajagopal, *Tetrahedron: Asymmetry* 2011, **22**, 857-865.

10- H. Li, M. Yang, X. Zhang, L. Yan, J. Li, Y. Qi, *New J. Chem*., 2013, **37**, 1343-1349.

11- Y. He, C. Cai, *Catal. Sci. Technol*., 2012, **2**, 1126-1129.

12- A. Schatz, M. Hager, O. Reiser, *Adv. Funct. Mater*., 2009, **19**, 2109-2115.

13- A. Schatz, R. N. Grass, Q. Kainz, W. J. Stark, O. Reiser, *Chem. Mater*., 2010, **22**, 305-310.

14- Sk. M. Islam, S. Mondal, P. Mondal, A. S. Roy, K. Tuhina, N. Salam, M. Mobarak, *J. Organomet. Chem*., 2012, **696**, 4264-4274.

15- G. Chouhan, D. Wang, H. Alper, *Chem. Commun*., 2007, 4809-4811.

16- R. B. Nasir Baig, R. S. Varma, *Chem. Commun*., 2012, **48**, 2582-2584.

17- B. Dragoi, A. Ungureanu, A. Chirieac, V. Hulea, S. Royerc, E. Dumitriua. *Catal. Sci. Technol.*, 2013, **3**, 2319-2329.

18- A. Corma, H. Garcia, A. Primo, *Journal of Catalysis* 2006, **241**, 123-131.

19- A. Biffis, E. Scattolin, N. Ravasiob, F. Zaccheria, *Tetrahedron Lett*., 2007, **48**, 8761-8764.

20- M. L. Shilpa, V. Gayathri, *Transition. Met. Chem*., 2013, **38**, 53-62.

21- M. Nandi, P. Roy, H. Uyamac, A, Bhaumik, *Dalton Trans*., 2011, **40**, 12510-12518.

22- V. Parvulescua, V. Niculescua, R. Enea, A. Popac, M. Mureseanud, C. D. Enee, M. Andruhe, *J. Mol. Catal. A: Chem*., 2013, **366**, 275-281.

23- M. Srinivasa, P. Srinivasua,, S. K. Bhargavab, M. L. Kantam, *Catalysis Today* 2013, **208**, 66-71.

24- T. Zeng, L. Yang, R. Hudson, G. Song, A. R. Moores, C. Jun. Li, *Organic Lett.,* 2011, **13** (3), 442-445.

25- V. G. Ramua, A. Bordoloib, T. C. Nagaiahc, W. Schuhmannc, M. Muhlerb, C. Cabrelea, *Appl. Catal., A*., 2012, **431-432**, 88-94.

26- M. Wang, P. Li, L. Wang, *Eur. J. Org. Chem*., 2008, 2255-2261.

27- B. Dervaux, F. E. Du Prez, *Chem. Sci*., 2012, **3**, 959-966.

28- K. B. Sharpless, V. V. Fokin, L. G. Green, V. V. Rostovtsev, *Angew. Chem.* 2002, **114**, 2708-2711; *Angew. Chem. Int. Ed*. 2002, **41**, 2596-2599.

29- T. Jin, M. Yan, Y. Yamamoto, *Chem. Cat. Chem*., 2012, **4** (9), 1217-1229.

30- N. Mukherjee, S. Ahammed, S. Bhadra, B. C. Ranu, *Green Chem*., 2013, **15**, 389-397.

31- Y. Monguchi, K. Nozaki, T. Maejima, Y. Shimoda, Y. Sawama, Y. Kitamura, Y. Kitadeb, H. Sajiki, *Green Chem*., 2013, **15**, 490-495.

32- F. Nadora, M. A. Volpeb, F. Alonsoc, A. Feldhoffd, A. Kirschninge, G. Radivoya, *Appl. Catal., A*., 2013, **455**, 39-45.

33- R. B. Nasir Baig, R. S. Varma, *Green Chem*., 2012, **14**, 625-632.

34- D. Wang, D. Astruc, *Chem. Rev.*, 2014, **114**, 6949–6985.

35- J. M. Collinson, J. D. E. T. Wilton-Ely, S. Diez-Gonzalez, *Chem. Commun*., 2013, **49**, 11358-11360.

36- L. Wan, C. Cai, *Catal Lett*, 2012, **142**, 1134-1140.

37- E. Moore, S. J. McInnes, A. Vogt, N. H. Voelcker, *Tetrahedron Lett*., 2011, **52**, 2327-2329.

38- T. Suzuka, Y. Kawahara, K. Ooshiro, T. Nagamine, K. Ogihara, M. Higa, *Heterocycles* 2012, **85**, 615-626.

39- J. Albadi, M. Keshavarz, *Synth. Commun.*, 2013, **43**, 2019-2030.

40- A. Megia-Fernandez, M. Ortega-MuÇoz, J. Lopez-Jaramillo, F. Hernandez-Mateo, F. Santoyo-Gonzaleza, *Adv. Synth. Catal*., 2010, **352**, 3306-3320.

41- E. Ozkal, S. Ozcubukcu, C. Jimeno, M. A. Pericas, *Catal. Sci. Technol*., 2012, **2**, 195-200.

42- T. Shamim, S. Paul, *Catal. Lett.*, 2010, **136**, 260-265.

43- J. M. Collinson, J. D. E. T. Wilton-Ely, S. Díez-Gonzalez, *Chem.Commun.*, 2013, **49**, 11358-11360.

44- A. Pourjavadi, S. H. Hosseini, S. S. Amin, *Chem. Eng. J.*, 2014, **247**, 85–92.

45- M. Chtchigrovsky, A. Primo, P. Gonzalez, K. Molvinger, M. Robitzer, F. Quignard, F. Taran, *Angew. Chem.*, 2009, **121**, 6030-6034.

46- Y. Wang, J. Liu, C. Xia, *Adv. Synth. Catal.*, 2011, **353**, 1534-1542.

47- U. Sirion, Y.J. Bae, B. S. Lee, D. Y. Chi, *Synlett*, 2008, **15**, 2326-2330.

48- J. Albadi, M. Keshavarz, F. Shirini, M. Vafaie-nezhad, *Catal. Commun.*, 2012, **27**, 17–20.

49- R. B. Nasir Baig and Rajender S. Varma, *Green Chem*., 2012, **14**, 625–632.

50- Y. M. A. Yamada, S. M. Sarkar, Y. Uozumi, *J. Am. Chem. Soc.*, 2012, **134**, 9285-9290.